Standard Ozone Profiles from Balloon and Satellite Data Sets

K. F. KLENK AND P. K. BHARTIA

Systems and Applied Sciences Corporation, Riverdale, MD

E. HILSENRATH AND A. J. FLEIG

Goddard Space Flight Center, Greenbelt, MD 20771

(Manuscript received 20 November 1982, in final form 16 July 1983)

ABSTRACT

Standard profiles based on upper level averaged profiles from BUV and lower level averaged profiles from balloon measurements are presented in a parametric representation as a function of time of year and latitude. The representation is a simple 4-parameter function representing the ozone amount (m-atm-cm) in each of 12 atmospheric layers defined following the standard Umkehr convention. The same parameterization is applied to the Nimbus-7 SBUV data and is compared to the BUV/balloon parameterization. The ozone variance unaccounted for by the representation is presented and discussed. The season–latitude representation reduces considerably the ozone variance at all levels and explains much of the correlation between layers. This simple representation and corresponding covariance matrix have been used as *a priori* information in the ozone vertical profile inversion of the Nimbus-7 SBUV experimental measurements.

1. Introduction

Standard ozone profiles were derived in this study to be used as *a priori* information for the Nimbus-7 Solar Backscattered Ultraviolet (SBUV) ozone profile inversion algorithm. These standard profiles are presented here because of their potential usefulness for other researchers in the verification of photochemical-dynamical stratospheric models, as *a priori* data for other remote sounders, or to provide a general climatology for ongoing comparisons with measurements.

The standard profiles derived here are based on the ozone profile results from the Nimbus-4 Backscattered Ultraviolet (BUV) experiment (as archived in *World Data Center A*, 1980) for the middle and upper stratosphere and on balloon measurements for the lower stratosphere and troposphere. Dütsch (1978) compiled a similar data set to study the vertical ozone distribution on a global scale. He used early BUV results and chemical-type balloon soundings including the United States Air Force Regener chemiluminescent sondes.

Other climatological ozone profiles also exist. However, they have been compiled exclusively from *in situ* soundings. The U.S. Standard Atmosphere Mid-Latitude Model (Krueger and Minzner, 1976) is a single ozone profile derived from 17 rocket soundings in the latitude range 45°N ± 15° combined with approximately 150 balloon soundings which were conducted in a latitude belt from 41° to 47°N mostly over North America. Hilsenrath and Dunn (1979) compiled a data set of nearly 7000 balloon soundings, worldwide for the period 1962–75 and computed average profiles for

various latitude zones and total ozone ranges up to an altitude of 10 mb. They also computed averaged upper stratospheric profiles for low, middle and high latitude zones using 77 optical and chemiluminescent rocket soundings. A significant difference exists between the average balloon and rocket profiles where they overlap. Hilsenrath and Dunn overcame this problem by accepting the balloon values as correct in absolute value and then extrapolating the balloon profile to higher altitudes using average scale heights based on the rocket profiles. They constructed a set of 21 standard profiles—3 for low latitudes, 8 for middle latitudes and 10 for high latitudes—by interpolating their averaged profiles to discrete total ozone amounts. Mateer *et al.* (1980) developed a similar set of 21 standard profiles for use in Umkehr retrievals using the rocket and balloon data compiled by Hilsenrath and Dunn. The major difference between the Mateer *et al.* profiles and the Hilsenrath and Dunn profiles was in the way the rocket and balloon overlap difference was resolved. Mateer *et al.* chose to accept the absolute ozone amounts from the rocket at the upper level and the balloon values at the lower levels but smoothly joined the balloon and rocket averaged profile in the mid-range, 5–20 mb for low and middle latitudes and 2–30 mb for the high latitudes.

The rocket data set used by these investigators as the basis for the ozone profile above 10 mb, consists of less than 100 soundings. Its coverage is too sparse to follow the seasonal and latitudinal variations in the upper stratosphere. The limitations of the balloon data set are less severe. The data set consists of 7000 sound-

ings and there is good coverage in space and time for the Northern Hemisphere extratropical latitudes. Balloon coverage, however, is sparse in the tropics and Southern Hemisphere. Nevertheless, the balloon data base provides the best available climatology from the surface to approximately 10 mb. We present in this paper a BUV/balloon ozone climatology which uses the balloon data set as the basis for the low-level climatology and the Nimbus-4 BUV data as the basis of the upper level profile.

2. Characteristics of the BUV data set

Before presenting the combined BUV/balloon climatology (Section 3), we will discuss some of the important characteristics of the BUV data set and present several averaged BUV profiles. For more details of the balloon data set, see Dütsch (1978) and Mateer *et al.* (1980).

a. BUV algorithm

The ozone vertical profiles derived from Nimbus-4 BUV radiances are obtained by the inversion of the radiative transfer integral equations. The algorithm is described by Bhartia *et al.* (1981). The algorithm attempts to minimize the differences between the observed and computed radiances by adjusting the ozone profile. The solution profile is one which also minimizes the departure from the first guess. The first guess ozone profile used by the BUV-algorithm is based on the climatologies of Mateer *et al.* (1980) and Hilsenrath and Dunn (1979) described in the Introduction.

b. Validity range

The altitude range where the BUV profile is determined primarily by the measured radiances, depends on several factors including the solar zenith angle, the total ozone amount and the shape of the ozone profile. This altitude range typically extends from 0.7 mb (50 km) to as low as 20–40 mb (22–26 km). Below the 20–40 mb altitude, the derived profile is determined primarily by the first guess profile. The altitude resolution is about 7–8 km. The BUV ozone vertical distribution is derived as a function of atmospheric pressure in contrast to rocket measurements where height is the primary independent variable. The physical processes giving rise to the backscattered radiance depend on the density of ozone relative to air density and except at very large solar zenith angles are independent of height. In order to specify the BUV ozone profile as a function of height, a height–pressure profile would be needed.

c. Coverage considerations

The BUV measurements were made from the Nimbus-4 satellite which was in a sun-synchronous orbit with a local noon equator crossing. The BUV profiles represent near local noon conditions at low and middle latitudes. At higher latitudes, in the summer where there is day-long sunshine, BUV retrievals are obtained in both the ascending and descending parts of the orbit. Thus the average for those latitudes represents a mixture of near noon and midnight profiles.

The near global nature and the continuous coverage of the BUV retrievals throughout the year are two important characteristics of the data set which make it ideal for computing standard profiles. There is an inhomogeneity in the spatial coverage in the equatorial region. The BUV experiment was affected by enhanced dark current when the satellite passed through the South Atlantic radiation anomaly. Therefore, vertical profiles in this region could not be obtained. Consequently, the averaged low latitude profiles obtained from BUV are representative primarily of the region from 50°E eastward to 150°W. The data gap extends to the middle latitudes of the Southern Hemisphere where it is located mainly from 110°W eastward to 20°W of the southern middle latitude region.

d. Error sources

The largest uncertainty in the ozone profiles derived from BUV is due to the ozone absorption coefficient errors. These are believed to be on the order of 3% for the profile wavelength bands (Klenk, 1980). This would cause errors of less than 6% in the ozone amounts. The uncertainty in the calibration of the instrument for measuring the ratio of the backscattered intensity to the incident solar flux is 2%. This translates into ozone error on the order of 3%. The nature of the constrained inversion is such that sharp features in the ozone profile are not resolved. The nature of this error is situation dependent.

e. Upper level averaged profiles

The seasonally averaged BUV profiles for each latitude zone of ozone mixing ratio versus atmospheric pressure are presented graphically in Figs. 1–3 and in tabular form in Tables 1–3. The averages include both Northern and Southern Hemisphere data for the same season, e.g., winter–north and summer–south are averaged together. The averaged profiles are computed for quarters centered about the solstices and equinoxes [see Frederick *et al.* (1983) for height–latitude cross sections of the BUV mass mixing ratio data average over three month intervals]. There are small differences usually on the order of a few percent (up to a maximum of 7%) between the northern and southern quarterly averages above 10 mb. These differences will not be explored in this paper.[1] The latitude bands are

---

[1] Northern–southern hemispherical differences are not large when quarterly averages are compared. However, Southern Hemisphere annual amplitudes above 3–4 mb, can be noticeably larger than those in the Northern Hemisphere.
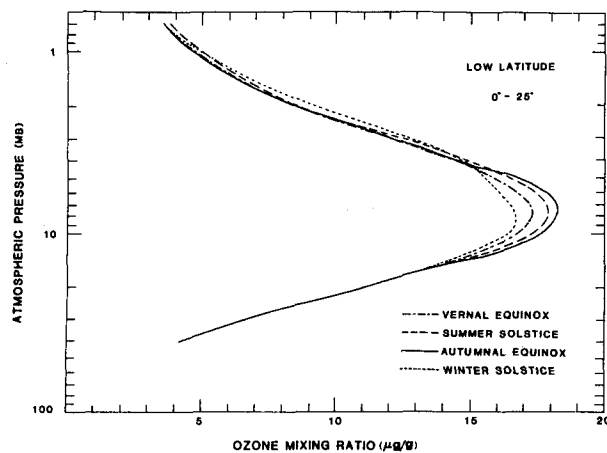
FIG. 1. Ozone mixing ratio versus atmospheric pressure
for the low latitude region < 25°.

FIG. 3. As in Fig. 1 but for high latitude region 65–80°.

defined as low (0–25°), middle (25–65°) and high (65–80°).

Note that the high latitude profile range extends to only 80°. This is the result of the nature of the Nimbus near polar sun-synchronous orbit which has a 99° inclination and thus the trace of the sub-satellite point is tangent to a latitude circle near 81°. The nadir viewing of the BUV instrument is limited to ±81° latitude.

The coverage in the high latitudes is seasonally dependent; BUV retrievals are performed for solar zenith angles in the field of view of up to 85.7°. Thus in the winter hemisphere at solstice, the highest latitude retrieval possible is at 63° latitude. Consequently, the coverage in the winter hemisphere high latitude band is too sparse to obtain a profile representative of the zone.

In Fig. 4 we compare the middle latitude annual-averaged BUV profile with that of Krueger and Minzner (1976), a commonly used climatological average middle latitude profile. The comparison is made in
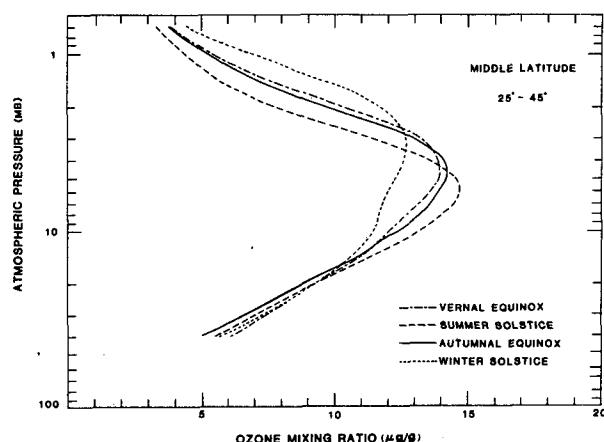
terms of the ozone mixing ratio versus pressure. The Krueger–Minzner profiles are seen to provide an annual mean profile consistent with the present results.

3. A time–latitude representation of the ozone profile

The ozone climatology presented in this section is a function of time (or day of year) and latitude. The climatologies of (Hilsenrath et al., 1979, and Mateer et al., 1980) were developed as a function of latitude band and a specified range of total ozone amounts. With the two parameters, latitude and total ozone, a considerable function of the ozone variance below the ozone density maximum can be explained. However,

FIG. 2. As in Fig. 1 but for the middle latitude region 25–45°.

TABLE 1. Low-latitude average profiles.

Level (mb)	Mixing ratio (μg g^{-1})*				
	Vernal equinox	Summer solstice	Autumnal equinox	Winter solstice	Annual
0.7	3.5	3.8	3.6	3.5	3.5
1.0	4.7	4.8	4.6	4.9	4.7
1.5	6.5	6.6	6.5	7.0	6.7
2.0	8.4	8.6	8.4	9.2	8.6
3.0	12.2	12.2	11.9	12.7	12.1
4.0	14.3	14.8	14.7	14.6	14.6
5.0	15.8	16.4	16.6	15.6	16.1
7.0	17.2	17.8	18.2	16.4	17.3
10.0	17.0	17.5	17.7	16.5	17.1
15.0	14.0	14.0	14.0	13.8	14.0
20.0	11.0	11.1	11.0	11.1	11.1
30.0	6.7	6.9	6.6	6.6	6.7
40.0	4.2	4.3	4.1	4.0	4.2
Total ozone (m-atm-cm)	259.7	268.0	263.0	251.7	260.6
Total samples	8060	8967	7604	8879	33 510
Average latitude	14.8	14.9	14.5	14.5	14.7

* To convert to ppm volume divide mixing ratio by 1.657.

TABLE 2. Middle latitude average profiles.

Level (mb)	Mixing ratio (μg g^{-1})*				
	Vernal equinox	Summer solstice	Autumnal equinox	Winter solstice	Annual
0.7	3.9	3.3	3.8	4.4	3.8
1.0	5.4	4.3	5.2	6.9	5.4
1.5	8.0	6.0	7.6	10.1	7.9
2.0	10.4	7.9	9.9	11.8	10.0
3.0	13.3	11.3	13.0	12.7	12.5
4.0	13.8	13.6	14.2	12.6	13.6
5.0	14.0	14.5	14.2	12.3	13.8
7.0	13.1	14.4	13.6	11.8	13.2
10.0	12.1	13.2	12.4	11.4	12.3
15.0	10.5	10.9	10.4	10.4	10.5
20.0	9.3	9.3	8.8	9.3	9.2
30.0	7.5	7.0	6.6	7.3	7.1
40.0	6.1	5.5	5.0	5.6	5.6
Total ozone (m-atm-cm)	365.3	332.7	302.5	325.2	331.8
Total samples	24 738	26 454	23 492	24 521	99 205
Average latitude	45.4	45.9	45.8	43.7	45.2

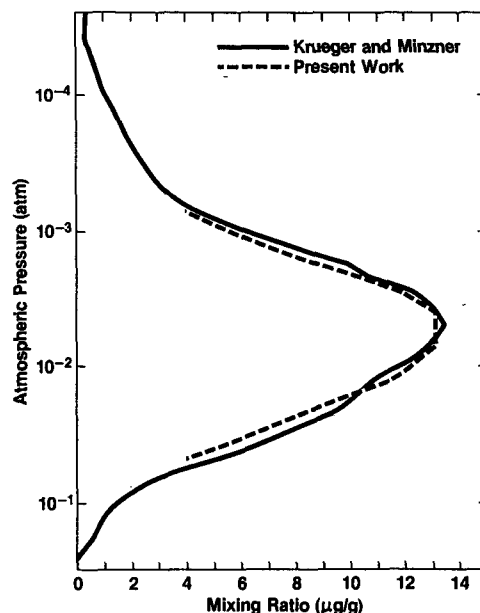* To convert to ppm volume multiply mixing ratio by 1.657.

FIG. 4. Comparison of annual averaged midlatitude ozone mixing ratio profile obtained from BUV with the Krueger and Minzner (1976) midlatitude profile.

for the levels above this, the ozone variation has little or no correlation with total ozone. For levels above the ozone density peak, the time of year becomes a significant predictor of the ozone amounts. The climatologies of Hilsenrath and Mateer, referred to earlier, being based on just a few rocket measurements could

TABLE 3. High latitude average profiles.

Level (mb)	Mixing ratio (μg g^{-1})*			
	Vernal equinox	Summer solstice	Autumnal equinox	Annual
0.7	3.8	2.8	3.6	3.1
1.0	5.1	3.8	5.5	4.5
1.5	7.5	6.1	7.8	6.6
2.0	9.5	7.4	9.4	8.3
3.0	11.5	10.2	10.6	10.5
4.0	11.9	11.4	10.6	11.4
5.0	11.7	11.5	10.3	11.2
7.0	10.5	10.3	9.0	10.0
10.0	8.9	7.7	7.5	8.3
15.0	7.6	7.1	6.2	7.0
20.0	7.1	6.5	5.7	6.4
30.0	6.5	5.9	5.1	5.7
40.0	6.0	5.5	4.8	5.4
Total ozone (m-atm-cm)	394.9	358.1	314.8	354.5
Total samples	8457	24 626	10 787	43 908
Average latitude	73.4	75.3	73.9	74.6

* To convert to ppm volume multiply mixing ratio by 1.657.

not define the seasonal and latitudinal ozone behavior in the upper stratosphere. The BUV measurements have made possible, because of the global and year-round coverage and the large number of measurements, a significantly better representation of the upper level ozone variability.

The ozone climatology presented in this section was developed to be used as *a priori* data in the Nimbus-7 SBUV ozone profile retrieval algorithm (Fleig *et al.,* 1982, and Schneider *et al.,* 1981). The covariance matrix associated with this climatology is discussed in the next section.

The climatology uses the first year of BUV data (April 1970–March 1971) for the ozone profile at altitudes above 15.6 mb and a balloon ozonesonde data set below. The balloon data set was obtained from the World Ozone Data Center (WODC), Atmospheric Environment Service (AES) of Canada in Toronto, Canada, containing soundings from 1965 to 1978. We did not include the United States Air Force Regener network sondes in our balloon averages.

The balloon data are most heavily concentrated in the middle latitudes of the Northern Hemisphere. Together the stations at Payerne (46°49′N) and Hohenpeissenberg (47°48′N) provided the majority of available soundings in this zone. Wallops Island (37°51′N), and Kagoshima (31°38′) and Tateno (36°03′N) are also well represented. The southern middle latitudes is mainly represented by the station at Aspendale (38°02′S). Soundings in the low latitudes are scarce. The dearth of data in the low latitudes led to some problems in the derivation of the climatology

which we discuss later in this section. The higher latitudes are represented mainly by the station in Resolute (74°43′N).

The BUV data set for the time period April 1970–March 1971 contains approximately 210 000 retrievals, representing one-third of the total seven-year BUV data set. We have used only the first year of BUV data in order to minimize the effect of the long-term drift which is present in the BUV data and the inhomogeneity in coverage characteristic of the later years.

For this analysis the atmosphere is divided according to the layering scheme used by the Umkehr network. Each layer, ∼5 km in thickness, is of sufficient resolution for expressing the detail in seasonal and latitudinal averages. It is also on the order of (although slightly smaller than) the resolution of the BUV technique. The lowest two layers which make up the troposphere have been combined into a single layer in this analysis. In the Umkehr layering scheme, the pressure at the bottom of the layer is twice the pressure at the top. The Umkehr layers are defined in Table 4.

A simple parametric representation of the time–latitude dependence of ozone includes an annual wave which decreases to zero at the equator and a latitude dependent factor. The representation used for each layer l, latitude λ, and day of the year t is given in the following expression for the layer ozone amount x^l.

$$x^l = a_0{}^l + [1 - \cos(2\lambda)]$$

$$\times \left\{ a_1{}^l + a_2{}^l \cos\left[(t - \phi^l) \frac{2\pi}{365} \right] \right\}. \quad (1)$$

The latitude λ is defined as −90° for the south pole and +90° for the north. The parameters a_0, a_1, a_2 and ϕ have simple interpretations. The parameter a_0 is the ozone amount at the equator which in this representation has no seasonal dependence; $2a_1$ is the measure of the equator to pole latitude dependence of the annual average ozone; a_2 is the amplitude of seasonal variation at 45° and ϕ is the day of the year the ozone reaches its annual maximum. For the Southern Hemisphere the seasonal variation is a half a year out of phase with

the north. Therefore when using (1) for the Southern Hemisphere 182.5 days should be added to the value of ϕ in Table 5.

The values of the parameters a_0, a_1, a_2 and ϕ are obtained by multiple linear regression against the Nimbus-4 BUV for layers 6 and above and against the WODC balloon data for layers 5 and below. In regressing the balloon data, we set the parameters a_0 equal to the low latitude averages of Hilsenrath and Dunn (1979). They were held constant in order to avoid unphysical ozone amounts in this region. Table 5 contains the parameter values for each atmospheric layer.

For the benefit of those investigators who have used the Krueger and Minzner profile, we compare it to the present climatology averaged over the year for a latitude of 45° in Fig. 5. [Eq. (1) reduces to $a_0 + a_1$ when averaged over the year at 45°.] The comparison is made in ozone partial pressure units (nanobars) in order to display the complete profile. The climatology developed here is plotted as a bar graph with each bar representing the averaged partial pressure in each Umkehr layer. It can be seen that the midlatitude profile of Krueger and Minzner compares closely to the averaged annual 45° profile derived from this work.

In order to demonstrate how (1) relates to the BUV data two sample comparisons are performed and illustrated in Figs. 6 and 7. In Fig. 6 ozone values computed from (1) for level 6 (15.6–7.8 mb) are compared to zonally averaged BUV data as a function of latitude. The time for the comparison is the week of the vernal equinox. The solid line represents the BUV observations and the dashed line the parametric values computed from (1). The main feature in this comparison is the strong latitude dependence of the ozone amount whose variation is fairly well represented by the parametric equation.

In the second comparison (Fig. 7) ozone values computed from (1) are compared to weekly zonally averaged BUV data as a function of time at 50°N. In this comparison the computed values appear as a sinusoid, agreeing well with the observations. The perturbation in the January observations is due to a stratospheric warming occurring at that time and is not well represented by the parametric equation. The warming, however, tends to decrease the annual amplitude somewhat leading to underestimation of the December ozone high.

Ozone values obtained from (1) for high latitude winter are not based on observation because BUV profiles cannot be retrieved in the polar night. Therefore, ozone values outside the BUV observation range derived from the parametric equation are only extrapolation and should be treated as such.

The parameterization, Eq. (1), represents the main features in the seasonal (annual wave) and latitudinal behavior of the ozone. The overall accuracy of the fit is 10%. Most of this error in layers 5–9 is due to real

TABLE 4. Umkehr layers.

Layer number	Pressure range (mb)
12	0.24–0.0
11	0.49–0.24
10	0.98–0.49
9	1.96–0.98
8	3.9–1.96
7	7.8–3.9
6	15.6–7.8
5	31.2–15.6
4	.62.5–31.2
3	125–62.5
2	250–125
1	1000–250

TABLE 5. Parameters for BUV/balloon climatology.

Layer	a_0 (m-atm-cm)	a_1 (m-atm-cm)	a_2 (m-atm-cm)	Day*
		from BUV data		
12	0.105	−0.007	0.004	0
11	0.25	0.01	0.04	−10
10	0.85	0.13	0.24	−11
9	3.0	0.62	0.99	−9
8	11.5	−0.40	0.7	4
7	33.0	−7.4	1.9	164
6	62.0	−19.0	2.4	154
		from balloon data		
5	75	−6	0	—
4	44	38	13	59
3	5	49	16	62
2	3	25	12	91
1	15	10	8	182

* For southern latitudes add 182.5 days.

systematic variations in the ozone which are not represented by Eq. (1); for example, semiannual waves, extrema in the latitudinal dependence not located at the pole or equator, and such sudden perturbations as the stratospheric warming.

Height–latitude cross sections of the ozone partial pressure using the BUV/balloon representation, Eq. (1), for four months—February, May, August and November, are shown in Figs. 8a–d. These figures can be used to compare directly to similarly drawn figures in Dütsch (1980).[2] Figs 8a, c and 8b, d are mirror images of one another since the presentation, Eq. (1), has hemispheric symmetry but a half-year out-of-phase. The cross sections were created by converting the ozone amounts in each layer using Eq. (1) and Table 5 to an average partial pressure. These cross sections exhibit all the prominent features seen in the Dutsch (1980) cross sections. A notable difference occurs in the high latitudes of the winter hemisphere where the BUV/balloon representation results in significantly higher (by 20%) ozone amounts at the ozone density maximum. This discrepancy reflects the general lack of observational data for this region and season.

We have compared the total ozone of this representation with the BUV derived total ozone zonal averages. The total ozone amount can be computed from Eq. (1) by summing all layers together. The time–latitude behavior of the total ozone from the BUV/balloon representation is plotted in Fig. 9. The values are very close to the BUV total ozone zonal averages reported by Heath *et al.* (1982) and Hilsenrath *et al.* (1979). Differences tend to be within ±10% of the BUV total ozone results. The exception to this is the
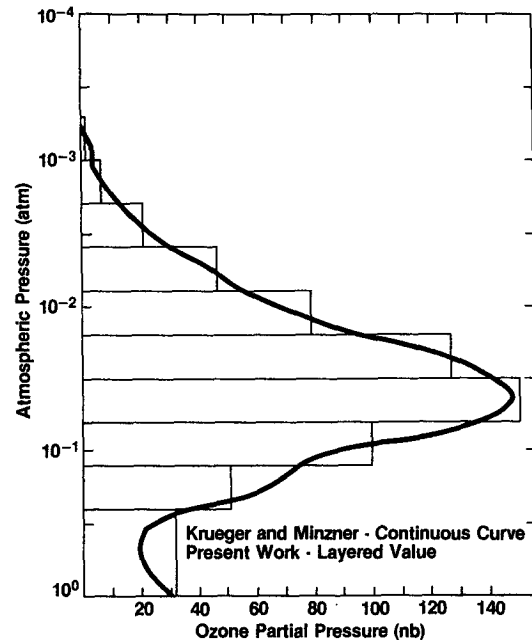
[2] See Figs. 6(a–d) of Dütsch (1980).

FIG. 5. Comparison of the annual averaged midlatitude ozone partial pressure profile at 45° obtained from Eq. (1) with the Krueger and Minzner (1976) midlatitude profile.

intensity of the spring maximum for the Southern Hemisphere which is known to be less intense than the Northern Hemisphere by as much as 20%. The spring maximum in Fig. 9 is near 480 d.u., which is typical in the Northern Hemisphere.

Ozone vertical profile results from the Nimbus-7 SBUV are also available. The SBUV ozone data have been derived with an inversion algorithm (Schneider *et al.*, 1981) which is a substantially improved version of that used for BUV. The BUV/balloon climatology
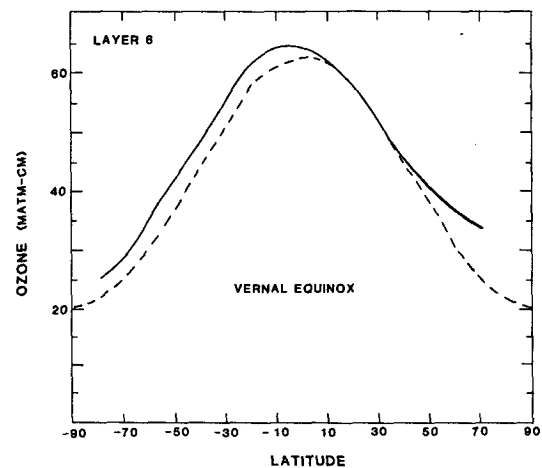

FIG. 6. Ozone amount in layer 6 versus latitude for the weekly averaged BUV data at vernal equinox, 1971. The BUV data (solid curve), the parametric representation (dashed curve).
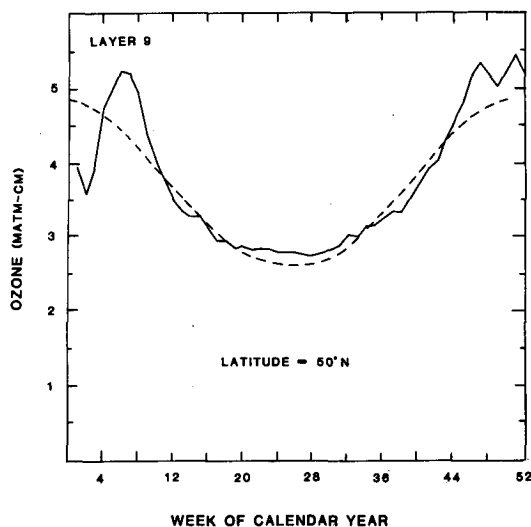
FIG. 7. Ozone amount in layer 9 versus week number of year 1971 for latitude 45°N. The solid curve is the BUV weekly averaged data and the parametric representation (dashed curve).

of Table 5 was used as the *a priori* constraint in the ozone inversion algorithm. With the SBUV data (as archived at the World Data Center-A for Rockets and Satellites in 1982) for the period November 1979 to October 1980, the parameters of Eq. (1) were derived and are shown in Table 6. For layers 6 and above, SBUV and BUV give similar climatologies.

An important result observed with the SBUV retrievals (Bhartia *et al.,* 1983) is that valid information on the ozone profile at levels below the ozone density maximum is being detected. Comparisons with monthly mean balloon measurements have shown that the departures of SBUV from the *a priori* ozone data agree with balloon measurements and can correctly track the seasonal ozone variation. Further analysis is needed in order to clearly define to what extent SBUV data at these levels can be used to supplement or replace the existing balloon measurements. The latitudinal and seasonal behavior of the SBUV lower level retrievals is presently being analyzed to see if Eq. (1) can be appropriately applied. Initial attempts to fit the lower
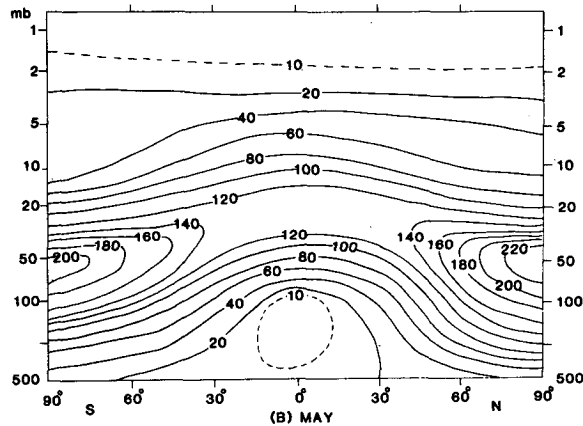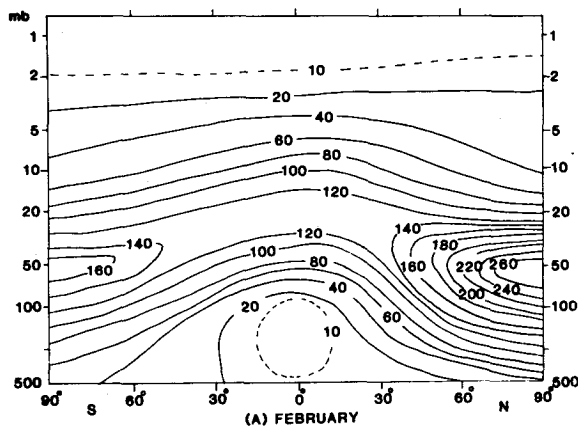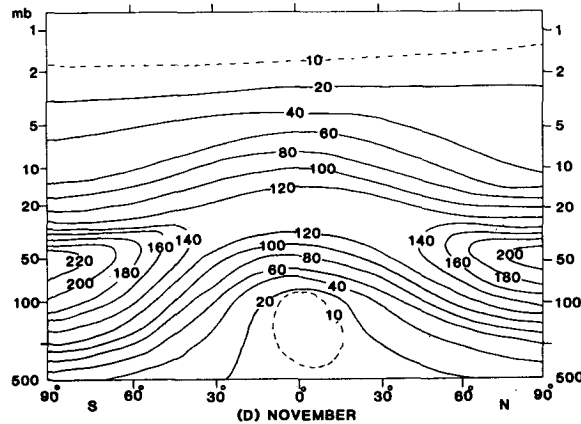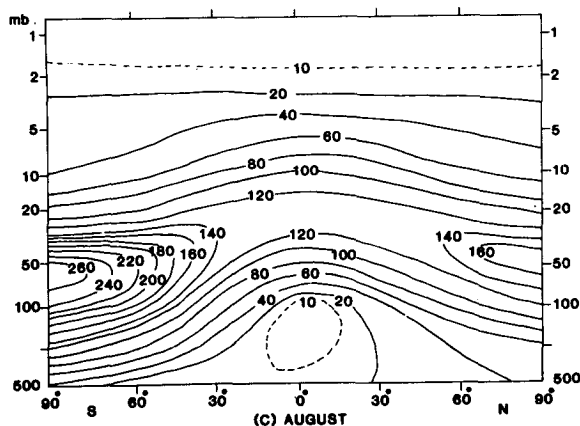

BUV/BALLOON

FIG. 8. Pressure (mb) versus latitude cross sections of the monthly averaged ozone partial pressure (nanobars) derived from Eq. (1) using parameter values in Table 5 for (A) February, (B) May, (C) August and (D) November.
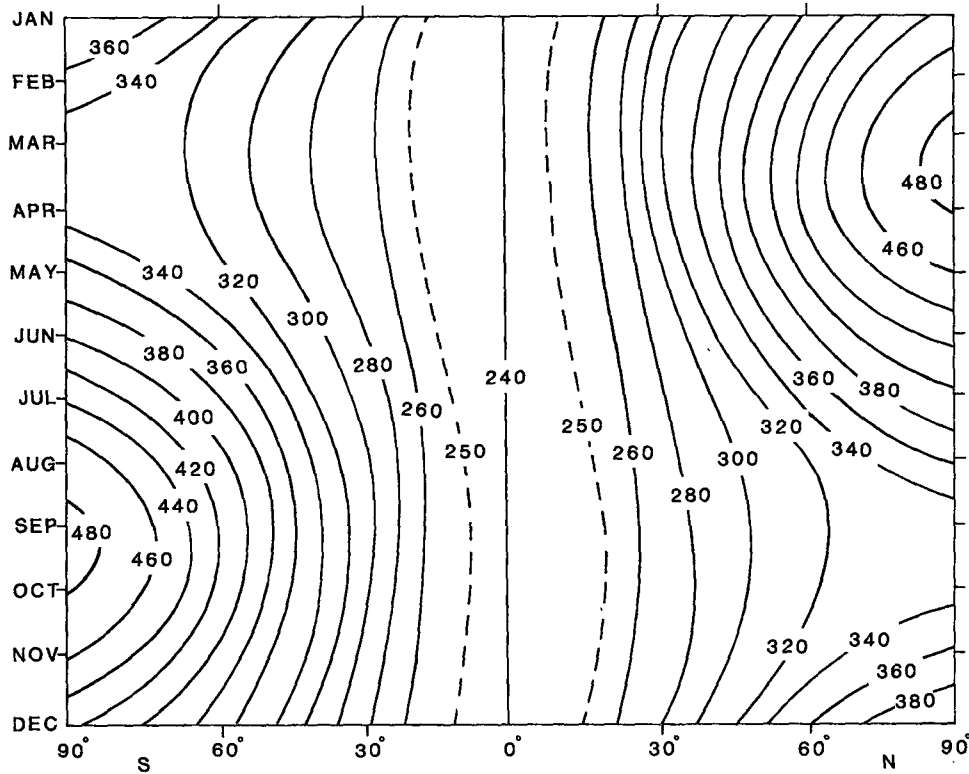
FIG. 9. Time–latitude contours of total ozone derived from Eq. (1)
using parameter values in Table 5. Total ozone units are m-atm-cm.

level SBUV data lead to underestimation of the latitudinal and seasonal parameters a_1 and a_2, respectively.

4. Ozone covariance matrix

The ozone covariance matrix is a symmetric matrix which describes the variance of ozone in each layer (diagonal elements) and the covariances (related to correlations) between two layers (off-diagonal elements). The covariance of layer l ozone X^l and layer m ozone X^m is $V_{l,m}$; it is computed from a set of observations X_i^l, $i = 1$, N and $l = 1$, L_N where N is the number of observations and L is the number of layers

TABLE 6. Parameters for SBUV climatology.

Layer	a_0 (m-atm-cm)	a_1 (m-atm-cm)	a_2 (m-atm-cm)	Day*
12	0.121	−0.011	0.003	16
11	0.284	0.003	0.034	−12
10	0.99	0.08	0.22	−15
9	3.36	0.42	0.93	−14
8	11.7	−0.6	0.6	0
7	32.3	−7.4	2.2	163
6	61	−20	3.6	160

* For southern latitudes add 182.5 days.

observed. The covariance $V_{l,m}$ in symbols is defined as

$$V_{l,m} = \frac{1}{N-1} \sum_{i=1}^{N} (X_i^l - \bar{X}^l)(X_i^m - \bar{X}^m). \qquad (2)$$

The quantity $\bar{X}^l$ can be defined in several ways. The meaning of the covariance depends on how $\bar{X}^l$ is defined. If $\bar{X}^l$ is defined as the average of the global set of ozone observations

$$\bar{X}^l = \frac{1}{N} \sum_{i=1}^{N} X_i^l, \qquad (3)$$

then $V_{l,n}$ represents the total covariance of the set of observations about the global average. If $\bar{X}^l$ is represented by the function of time and latitude in (1), then the variance and covariance represent only the part of the total variance and covariance of the set of observations that remains after the functional dependence of (1) is subtracted from the observations. In the discussion that follows, we will compare the variances for several climatologies or definitions of $\bar{X}_l$.

a. Fractional standard deviation

The variance of the ozone in layer l is the diagonal element $V_{l,l}$

$$V_{l,l} = \frac{1}{N-1} \sum_{i=1}^{N} (X_i{}^l - \bar{X}^l)^2. \qquad (4)$$

The fractional variance $v_{l,l}$ and fractional standard deviation σ_l are defined as

$$\sigma_l{}^2 = v_{l,l} = \frac{V_{l,l}}{\bar{X}^{l2}} = \frac{1}{N-1} \sum_{i=1}^{N} \left(\frac{\Delta X_i{}^l}{\bar{X}^l} \right)^2, \qquad (5)$$

where

$$\Delta X_i{}^l = X_i{}^l - \bar{X}^l. \qquad (6)$$

The quantity in parentheses in the equation above is the ozone difference expressed as a fraction of the average ozone in the layer. The fractional standard deviation is conceptually easier to understand when discussing the numerical values. For example, $\sigma_l = 0.1$ means that the standard deviation of the ozone in layer l is 10% of the average ozone in that layer.

In Fig. 10, we compare the fractional standard deviations for the following climatologies.

1) *Mateer's Global Climatology* (solid bars). This climatology as described in the Introduction is based on the balloon and rocket (UV optical type) observations (Mateer *et al.*, 1980). We converted the variances presented in Table 9a and Table 13 of Mateer *et al.* into fractional standard deviations. These values represent the global variation of the *in situ* measure-

ments themselves. In terms of Eqs. (5) and (6), $\bar{X}^l$ is the global average of the *in situ* measurements—rocket for layers 6–9 and balloons for layers 1–5.

2) *Global BUV* (bars with "B"). This is the global variation observed from the Nimbus-4 BUV from a full year of observations.

3) *Mateer Global with Total Ozone* (short dashed bars). This climatology assumes that the total columnar ozone amount is precisely known. The reduction in variance achieved by knowing the total ozone value is computed using the correlation between total ozone and the ozone layer amount. We computed the fractional standard deviation using the covariance matrix in Table 9b of Mateer *et al.* (1980).

4) *Middle Latitude with Total Ozone and Latitude* (hollow dotted bars). The climatology of Hilsenrath and Dunn (1979) averaged profiles into 50 m-atm-cm bins and latitude zones. The hollow dotted bars represented the fractional standard deviations of ozone in the middle latitude zone (25°–55°) when the total ozone is known (to a precision of roughly ±25 m-atm-cm). This example is intended to show how well latitude and ozone together can be used to predict layer ozone amounts.

5) *Latitude and Time* (dashed bars). The fractional standard deviations of ozone about the parameterization of (1) show how effective latitude and time are as predictors of the layer ozone amounts.
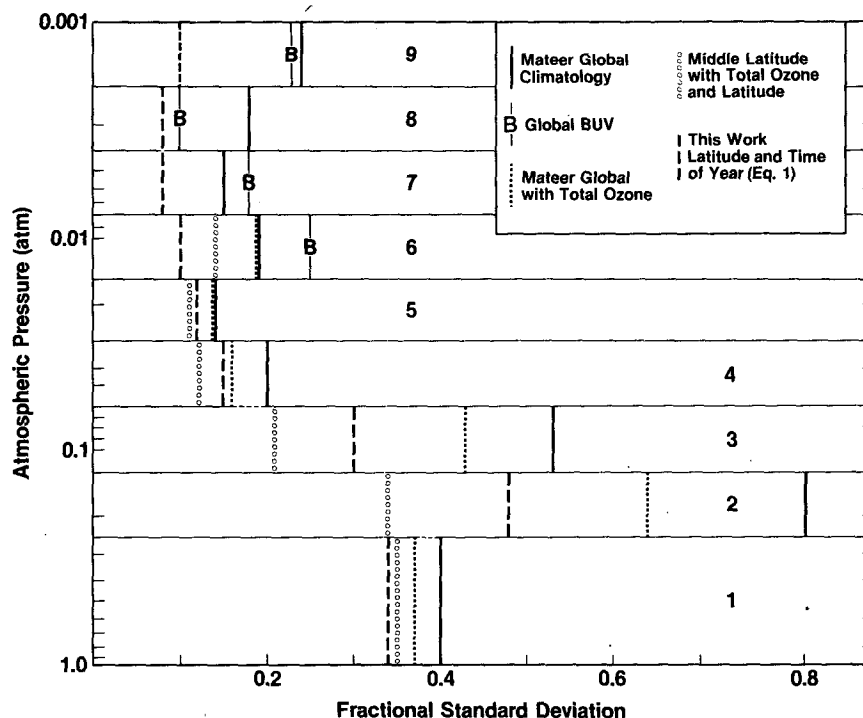

FIG. 10. Bar chart illustrating the fractional standard deviation of ozone amount in Umkehr layers for several climatologies derived from observational data.

Figure 10 shows that the time and latitude representation of Eq. (1) is an effective predictor of layer ozone amount for all layers and in particular for layers 4–9 where the unexplained variances are 15% or less. In the lower stratosphere layers 2–4, latitude and total ozone are effective predictors of layer ozone amounts.

We summarize Fig. 10 as follows: 1) for layers 6 through 9, the time of year and latitude via (1), dashed bars, is a 10% accurate predictor of the layer ozone amount; 2) for layers 2 through 4, total ozone (accurate to ±25 m-atm-cm) and latitude zone (i.e., low, middle, or high) is a 10–30% predictor of the layer ozone amount and more effective than Eq. (1); and 3) in layer 5 either time–latitude or total ozone–latitude is an equally effective indicator of the ozone amount (~12%).

b. Correlations between layers

We define the covariance $v_{l,n}$ of the fractional ozone differences as

$$v_{l,m} = \frac{V_{l,m}}{\bar{X}_l \bar{X}_m} = \frac{1}{N-1} \sum_{i=1}^{N} \frac{\Delta X_i^l}{\bar{X}^l} \frac{\Delta X_i^m}{\bar{X}^m} . \quad (7)$$

The correlation coefficient $r_{l,n}$ between the layer l and m fractional ozone differences is

$$r_{l,m} = \frac{r_{l,m}}{\sigma_l \sigma_m} . \quad (8)$$

The correlation coefficient is a measure of how the ozone in two different layers, at a given location and time, vary relative to one another. The correlation coefficients are given in Table 7 for the ozone variation remaining after variation represented in Eq. (1) is removed. Most of the correlation and anticorrelation between layers is due to the annual and latitudinal variations which are accounted for in Eq. (1). Inspection of the pressure versus latitude cross sections in Fig. 8, illustrate the existence of significant layer correlation in how the patterns change from season to season. The correlations in Table 7 represent the residual correlation remaining after the annual and latitudinal correlations between layers is removed via Eq. (1). These correlation coefficients defined in this way are necessary for the optimum statistical inversion technique used to derive ozone profiles from SBUV.

5. Conclusion

The Nimbus-4 BUV experiment resulted in a unique data set in that it provided a global perspective of seasonal ozone variations. The climatology of zonally averaged ozone presented in this paper is a convenient time and latitude representation of the ozone which may be useful for theoretical and experimental studies

TABLE 7. Correlations between layer ozone amounts with seasonal and latitudinal behaviors removed using Eq. (1).

	Neighbor	Next-neighbor
9		
	0.52	
8		−0.09
	0.34	
7		−0.13
	0.50	
6		0.00
	0.48	
5		0.00
	0.56	
4		−0.01
	0.39	
3		0.10
	0.61	
2		0.06
	0.31	
1		

of the stratosphere. Because of the extensive coverage of the satellite data, this climatology is superior to those previously available which utilize only *in situ* soundings, particularly in the upper stratosphere.

The SBUV ozone data set which is presently being developed will be a stable, multiyear ozone data set. The ozone retrieval technique used for SBUV is superior to the BUV technique especially in its ability to derive ozone information in layer 5 and below. The SBUV data set will provide a unique opportunity to improve upon the climatology presented here. There is room for improvement in our understanding of the global ozone variation. One area is the high latitude winter region where little observational information is available. Another area is the tropics and, in particular, below the ozone maximum where balloon measurements could provide information.

REFERENCES

Bhartia, P. K., K. F. Klenk, V. G. Kaveeshwar, S. Ahmad, A. J. Fleig, R. D. McPeters and C. L. Mateer, 1981: Algorithm for vertical ozone profile determination for the Nimbus-4 BUV data set *Preprints Fourth Conf. on Atmospheric Radiation*, Toronto, Amer. Meteor. Soc., 27–32.
——, ——, A. J. Fleig, C. G. Wellemeyer and D. Gordon, 1984: Intercomparison of Nimbus-7 Solar Backscattered Ultraviolet (SBUV) ozone profiles with rocket, balloon and Umkehr profiles. *J. Geophys. Res.* (in press).
Dütsch, H. U., 1978: Vertical ozone distribution on a global, *Pure Appl. Geophys.*, **116**, 511–529.
Fleig, A. J., K. F. Klenk, P. K. Bhartia, K. D. Lee, C. G. Wellemeyer and V. G. Kaveeshwar, 1981: Vertical ozone profile results

from the Nimbus-4 BUV data," *Preprints Fourth Conf. on Atmospheric Radiation,* Amer. Meteor. Soc., 20–26.

——, ——, ——, D. Gordon and W. H. Schneider, 1982: *User's Guide for the Solar Backscattered Ultraviolet (SBUV) Instrument First-Year Ozone-S Data Set,* NASA Reference Publication 1095 [Available from NTIS]., 72 pp.

Frederick J. E., F. T. Huang, A. R. Douglass and C. A. Reber, 1983: The distribution and annual cycle of ozone in the upper stratosphere, *J. Geophys. Res.,* **88,** 3819–3828.

Heath, D. F., A. J. Fleig, A. J. Miller, T. G. Rogers, R. M. Nagatani, H. D. Bowman II, V. G. Kaveeshwar, K. F. Klenk, P. K. Bhartia and K. D. Lee, *Ozone climatology series. Atlas of Total Ozone. April 1970–December 1976,* Vol. 1, NASA Ref. Pub. 1098, 178 pp. [Available from NTIS].

Hilsenrath, E., and P. J. Dunn, 1979: Standard profiles for total ozone retrievals. (Unpublished).

——, D. F. Heath and B. M. Schlesinger, 1979: Seasonal and interannual variations in total ozone revealed by the Nimbus-4 Backscattered Ultraviolet Experiment, *J. Geophys. Res.,* **84,** 6969–6979.

Krueger, A. J., and R. A. Minzner, 1976: A Mid-latitude ozone model for the 1976 U.S. Standard Atmosphere. *J. Geophys. Res.,* **81,** 4477–4481.

Mateer, C. L., J. J. DeLuisi and C. C. Porco, 1980: The short Umkehr method, Part I: Standard ozone profiles for use in the estimation of ozone profiles by the inversion of short Umkehr observations. NOAA Tech. Memo. ERL ARL-86, 20 pp.

Schneider, W. H., P. K. Bhartia, K. F. Klenk and C. L. Mateer, 1981: An optimum statistical technique for ozone profile retrieval time backscattered UV radiances. *Preprints Fourth Conf. on Atmospheric Radiation,* Toronto, Amer. Meteor. Soc., 33–37.